ELSEVIER

Earth and Planetary Science Letters 205 (2003) 257–271

EPSL

www.elsevier.com/locate/epsl

Neotectonic modelling of the western part of the Africa–Eurasia plate boundary: from the Mid-Atlantic ridge to Algeria

Ivone Jiménez-Munt [a,*], Ana M. Negredo [b]

[a] *Department of Earth Sciences, Section of Geophysics, University of Milan, Via Cicognara 7, 20129 Milan, Italy*
[b] *Department of Geophysics, Faculty of Physics, University Complutense of Madrid, Av. Complutense, 28040 Madrid, Spain*

Received 16 July 2002; received in revised form 10 October 2002; accepted 22 October 2002

Abstract

In this work we use the thin-shell approximation to model the neotectonics of the western part of the Africa–Eurasia plate boundary, extending from the Mid-Atlantic ridge to Tell Atlas (northern Algeria). Models assume a nonlinear rheology and include laterally variable heat flow, elevation, and crust and lithospheric mantle thickness. Including the Mid-Atlantic ridge permits us to evaluate the effects of ridge push and to analyse the influence of the North America motion on the area of the Africa–Eurasia plate boundary. Ridge push forces were included in a self-consistent manner and have been shown to exert negligible effects in the neotectonics of the Iberian Peninsula and northwestern Africa. Different models were computed with systematic variation of the fault friction coefficient. Model quality was scored by comparing predictions of anelastic strain rates, vertically integrated stresses and velocity fields to data on seismic strain rate computed from earthquake magnitude, most compressive horizontal principal stress direction, and seafloor spreading rates on the Mid-Atlantic ridge. The best model scores were obtained with fault friction coefficients as low as 0.06–0.1. The velocity boundary condition representing spreading on the Mid-Atlantic ridge is shown to produce concentrated deformation along the ridge and to have negligible effect in the interior of the plates. However, this condition is shown to be necessary to properly reproduce the observed directions of maximum horizontal compression on the Mid-Atlantic ridge. The maximum fault slip rates predicted by the model are obtained along the Mid-Atlantic ridge, Terceira ridge and Tell Atlas front. Relatively high slip rates are also obtained in the area between the Gloria fault and the Gulf of Cadiz. We infer from our modelling a significant long-term seismic hazard for the Gloria fault, and interpret the absence of seismicity on this fault as possibly due to transient elastic strain accumulation. The present study has also permitted better understanding of the geometry of the Africa–Eurasia plate boundary from the Azores triple junction to the Algerian Basin. The different deformational styles seem to be related to the different types of lithosphere, oceanic or continental, in contact at the plate boundary.

Keywords: stress; strain rate; seismicity; fault friction coefficient; diffuse plate boundary; Gloria fault

* Corresponding author. Tel.: +39-2-50-31-84-81; Fax: +39-2-50-31-84-89.
E-mail addresses: ivone.jimenez@unimi.it (I. Jiménez-Munt), anegredo@fis.ucm.es (A.M. Negredo).

0012-821X/02/$ – see front matter © 2002 Elsevier Science B.V. All rights reserved.
PII: S0012-821X(02)01045-2

1. Introduction

Differential movement between Eurasia, Africa and Iberia during the opening of the North Atlantic created lines of weakness that afterwards acted as plate boundaries [1,2]. The Mid-Atlantic ridge, which is marked by its morphology, seismicity and magnetic anomalies, is more sharply defined than the Africa–Eurasia plate boundary, which trends east–west and extends from the Azores triple junction into the Mediterranean Sea (Fig. 1).

Geophysical studies of the Azores triple junction suggest that the spreading rate of the Mid-Atlantic ridge south of the Azores Islands is lower than that observed in the northern segment, which results in a dextral transcurrent movement along the boundary.

Plate kinematics studies and earthquake fault plane solutions show the tectonic regime of the Africa–Eurasia plate boundary to change progressively from a small component of extension at its western end [3], through pure right lateral strike-slip at the Gloria fault (e.g. [2,4,5]). In the continental domain (east of the Madeira Tore Rise), active tectonics together with the seismicity distribution support an oblique plate convergence and the existence of a wide transpression zone from Gorringe, across the Alboran Sea, to the Tell Atlas mountains [6].

The Azores segment has high seismicity of moderate magnitude and a relatively low slip rate; the predominant mechanism is normal or transform faulting with horizontal tension axes averaging N25°E [5]. The Gloria fault (from 24°W to 20°W) forms a very clear seismic gap. From 20°W to 13°W the boundary is E–W oriented, currently marked by an alignment of large right lateral strike-slip earthquakes. However, the area of the Gorringe Bank is more complex, with reverse faulting as the predominant mechanism with N30°W horizontal pressures [4,5]. Further to the east, seismotectonic studies show a change in the tectonic regime from strike-slip and normal faulting in the Alboran Sea and Betic–Rif cordillera, to reverse faulting in the Tell Atlas [7,8].

Two recent studies have investigated the neotectonics of the Africa–Eurasia plate boundary between the eastern end of the Terceira ridge and the Gibraltar Arc [9] and in the Ibero–Maghrebian region (southern part of the Iberian Peninsula and northwestern Africa) [10]. In the present modelling we integrate results from these studies concerning the geometry of the plate

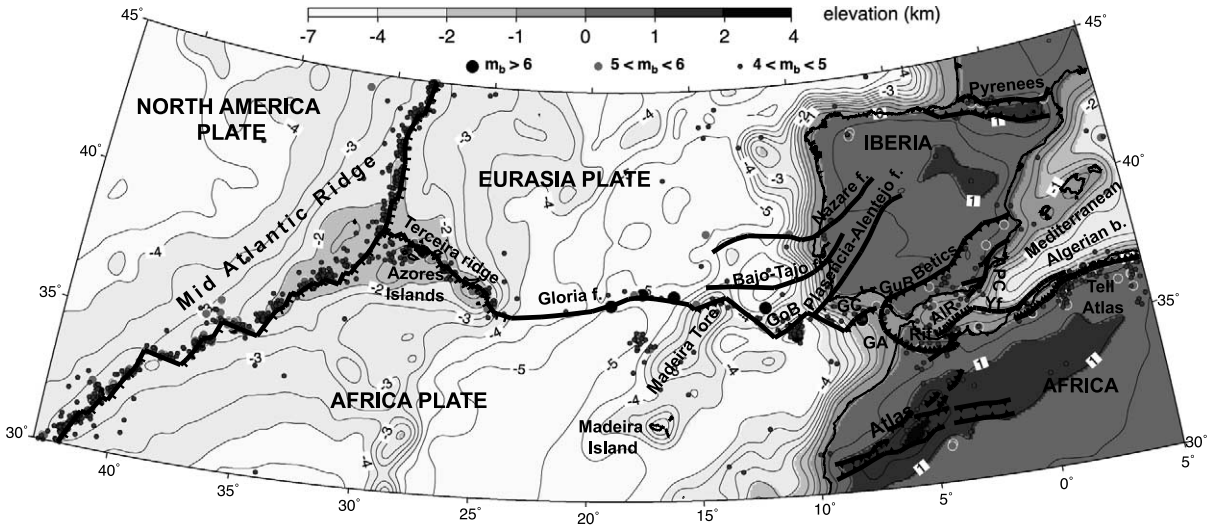

Fig. 1. Tectonic sketch map, elevation (ETOPO5) and seismicity (CNSS) of the study region. GoB, Gorringe Bank; GC, Golf of Cadiz; GuB, Guadalquivir Bank; GA, Gibraltar arc; AlR, Alboran ridge; APC, Alhama–Palomares–Carboneras fault system; Yf, Yussuf fault; f., fault; b., basin.

boundary, and we enlarge the model domain to include the Mid-Atlantic ridge, the Azores Islands, the whole Iberian Peninsula and Tell Atlas mountains (Fig. 1). Including the Mid-Atlantic ridge will permit us to analyse possible ridge push effects on the modelled area, and to study the influence of the North America motion on the area of the Africa–Eurasia plate boundary. Moreover, this novelty will enable us to incorporate data on seafloor spreading rates on the Mid-Atlantic ridge to score different models. In the eastern part of the study area, model-predicted stress orientations in the Iberian Peninsula will be compared to results of recent microstructural and seismological analysis [11]. Furthermore, predictions of horizontal velocity distribution in the Iberian Peninsula will be compared to preliminary geodetic estimations available in the area.

Estimations of fault slip rates will provide indications of their relative long-term seismic hazard. In this sense, another significant novelty of this study is that we will investigate possible reasons for the absence of instrumental seismicity on the Gloria fault, a striking feature relevant for seismic-hazard assessment due to its proximity to populated Azores Islands.

Such an extended model domain will permit us to study a boundary that presents (from west to east) extension, strike-slip and compression, and that separates oceanic–oceanic, continental–continental, and continental–young oceanic (Algerian basin) types of lithosphere. We also intend to better constrain the geometry of the plate boundary in the study area, where it is more poorly described.

2. Methodology

In the present study we have used the thin-shell finite element program SHELLS introduced by Kong and Bird [12] (see also [13] for information about the availability of several thin-plate and thin-shell freeware codes). The thin-shell modelling method is based on the approximation that horizontal velocity components are independent of depth in the lithosphere. A two-dimensional finite element grid is used to solve only the horizontal components of the momentum equation, whereas the radial (vertical) component of the momentum equation is represented by the isostatic approximation. Therefore, only the horizontal components of the velocity are calculated. Vertical normal stress is given by the weight of overburden per unit area, and flexural effects are neglected. Some characteristics of three-dimensional methods are incorporated into this method, since volume integrals of density and strength are performed numerically in a lithosphere of laterally varying crustal and lithospheric mantle thicknesses.

This method solves for anelastic deformation and transient effects such as elastic strain and earthquake cycle are neglected. Therefore, model-predicted steady velocities, fault slip rates and stresses should be considered as averages over several seismic cycles. The models assume a nonlinear rheology. Given a current strain rate tensor, the deviatoric stress tensor is calculated at many test points throughout the volume of the lithosphere using both frictional-sliding and dislocation-creep flow laws. The mechanism giving the lower maximum shear stress is assumed to dominate at that point. Frictional faulting stress, σ_f, is calculated under the assumption of hydrostatic pore pressure and no cohesion:

$$\sigma_f = \mu_f(-\sigma_n - P_w)$$

where μ_f is the coefficient of friction, σ_n is normal stress and P_w is the pore pressure. The two-dimensional finite element grid consists of continuum and fault elements. The friction coefficient is assumed to be 0.85 in continuum elements, whereas a lower value is assigned in fault elements. The following equation for the dislocation-creep (power law) rheology has been applied:

$$\tilde{\sigma} = \left[2A\,(2\sqrt{-\dot{\varepsilon}_1\dot{\varepsilon}_2-\dot{\varepsilon}_1\dot{\varepsilon}_3-\dot{\varepsilon}_2\dot{\varepsilon}_3})^{(1-n)/n}\exp\left(\frac{B+Cz}{T}\right)\right]\tilde{\dot{\varepsilon}} \quad (2)$$

where $\tilde{\sigma}$ is the deviatoric stress tensor $\tilde{\dot{\varepsilon}}$ is the anelastic strain rate tensor, T is absolute temperature, and z is depth. The rheologic parameters adopted for the crust/mantle are: $A = 2.3\times10^9/9.5\times10^4$ Pa $s^{1/3}$; $B = 4000/18314$ K; $C = 0/0.017$ K m^{-1}; $n = 3/3$. Values for the crust are taken from the neotectonic models by Bird and Kong

[14], and those of the mantle from the studies of olivine deformation by Kirby [15]. A detailed study of the model sensitivity to changes in these rheologic parameters is presented by Negredo et al. [10].

3. Modelling inputs

3.1. Grid geometry

The finite element grid used for modelling consists of 5694 triangular continuum elements and 365 fault elements. Only mapped fault zones thought to be active or potentially active are considered in our modelling (Fig. 1). Some fault elements do not represent individual faults, but zones of faults. We assign a dip to each fault element. Where dip cannot be inferred from geologic or geophysical data, we assign a dip of 25° for thrusts, 65° for normal faults, and 90° for strike-slip faults. These assigned values do not determine the slip sense of the corresponding fault, only vertical faults are forced to have strike-slip motion. Likewise, any fault which is not sufficiently stressed may remain locked.

The set of faults considered for the Ibero–Maghrebian region (from 10°W to 5°E) derive from the neotectonic modelling of this region by Negredo et al. [10]. We have incorporated in the present study those faults that were relatively active in their best fitting model. The main characteristic of that model is that the Africa–Eurasia plate boundary branches in the Ibero–Maghrebian region along the Betics and Rif–Tell thrust front. To the west of the Gibraltar Arc we have included a thrust fault following the Guadalquivir Bank, recently mapped in new multichannel seismic profiles [16]. Faults in the western Iberian Peninsula and their prolongation into the Iberian Atlantic margin are taken from Buforn et al. [5]. The modelled plate boundary between 10°W and 25°W is similar to that considered in the neotectonic study by Jiménez-Munt et al. [9]; it roughly follows the Gorringe Bank, the northern part of the Madeira Tore Rise and the Gloria fault. Further to the west, the modelled plate boundary follows the Terceira ridge to finally join the Mid-Atlantic ridge at the Azores triple junction. The geometry of the Africa–Eurasia plate boundary to the west of 10°W and that of the Mid-Atlantic ridge have been taken from the work of the Paleo-Oceanographic Mapping Project at the University of Texas Austin.

3.2. Heat flow and lithospheric structure

To determine the crustal and lithospheric mantle structure we assumed local isostasy and a steady-state thermal regime, defining the base of the lithosphere as the 1300°C isotherm. Under these conditions, we used elevation and surface heat flow as input data to determine the lithospheric structure (crustal and lithospheric mantle thickness) in the whole region. Elevation was obtained from the ETOPO-5 digital dataset, with data every 5′ of arc (Fig. 1). Surface heat flow was taken from the global dataset of Pollack et al. [17], supplemented by the data obtained by Fernàndez et al. [18] for the Iberian Peninsula and its margins and the western Mediterranean. Since there are very few heat flow measurements in the oceanic domain, we use the heat flow–age relationship proposed by Parsons and Sclater [19]. We consider the magnetic anomalies from the Mid-Atlantic ridge to near the M0 anomaly, so lithospheric ages range from the present to 118 Ma. We assumed a maximum surface heat flow of 250 mW m^{-2} on the Mid-Atlantic ridge. Fig. 2 shows the result of combining all these surface heat flow data. This figure shows the increasing surface heat flow towards the ridge, that results from a thinning of the lithospheric mantle. Also in the western Mediterranean, the high measured heat flow is associated with a significant lithospheric thinning in the Alboran Sea and Algerian basin [20]. The crustal and lithospheric mantle parameters used to determine the thickness of both layers are: density of 2780/3386 kg m^{-3} at 0 K, volumetric thermal expansion coefficient of $0/3.5\times10^{-5}$ K^{-1}, a thermal conductivity of 3.0/3.2 W m^{-1} K^{-1} and a radioactive heat production of $7.91\times10^{-7}/0$ W m^{-3}.

The calculations have been performed after filtering elevation and heat flow data, to remove local features. However, the adopted spatial reso-

lution is adequate to obtain important lateral variations in the total lithospheric strength and in the gravitational potential energy.

3.3. Boundary conditions

The applied boundary conditions are shown schematically in Fig. 2. We adopt the poles and rotation velocities for Africa and America obtained by Argus et al. [21] to impose boundary conditions that reproduce the motion of these plates with respect to a fixed Eurasia plate. Therefore, no motion is allowed in the northern boundary. The southern boundary and the southern part of the eastern boundary (from 30°N to the Tell thrust front) are assigned velocities of the Africa plate. Therefore we assume that regions outside these boundaries are rigid parts of the Africa plate. The northeastern boundary (from the Tell Atlas front to 45°N) is allowed to move, with normal tractions given by local lithostatic pressure. We have tried two different types of boundary conditions along the Mid-Atlantic ridge (MAR) resulting in two model sets hereinafter named 2_PLATES and 3_PLATES. In the first model set we only consider the interaction between Africa and Eurasia and apply to the boundary corresponding to MAR the same condition as to the northeastern boundary, with lithostatic pressure computed at MAR. In the second model set, fault elements, characterised by double nodes, are defined all along the boundary corresponding to MAR. Velocity conditions representing the motion of the North America plate with respect to Eurasia are applied to the outside of fault elements along the ridge. The velocity calculated for nodes along MAR that belong to Africa and Eurasia will depend on the fault friction coefficient, also resulting in different spreading rates. Therefore the velocity of North America is not transmitted directly to Africa and Eurasia plates. Model set 3_PLATES will permit us to study the effects of the interplay between three tectonic plates on the study area.

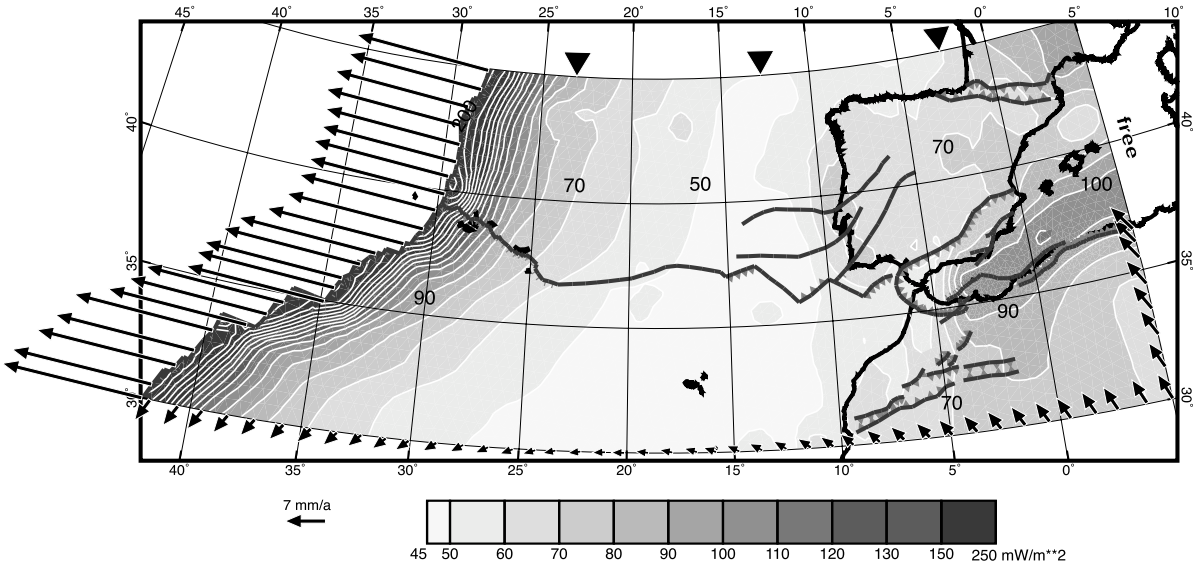

Fig. 2. Surface heat flow distribution (mW m^{-2}) obtained from data of Pollack et al. [17] and Fernàndez et al. [18], and from the oceanic age–heat flow relations from Parson and Sclater [19]. Contours every 5 mW/m^2. Black symbols represent the boundary conditions used in the 3_PLATES model set. Note that velocities applied at the ridge are only imposed to the nodes belonging to the North America plate, while the velocities at the nodes along the ridge that belong to Africa and Eurasia will be computed by the models. On the western boundary of 2_PLATES model set the condition is of lithostatic pressure.

4. Results and discussion

4.1. Scoring the quality of results

For each set of models, we vary systematically the fault friction coefficient from 0.01 to 0.85. In order to select the best model, we compare model predictions to the strain rate calculated with seismological data (Fig. 1), the observed directions of maximum horizontal compression (Fig. 3), and the spreading rates on the Mid-Atlantic ridge obtained from the magnetic anomalies (Fig. 3). Another possible testable result would be the relative velocity between different points of the model. However, as will be discussed later, we cannot perform yet a quantitative comparison due to the short time span of geodetic measurements in the area.

To score the predicted strain rates, we have followed the procedure described by Jiménez-Munt et al. [22] to calculate a normalised coefficient of correlation between the seismic strain rate and the modelled maximum principal strain rate. The seismic strain rate has been calculated using the methodology described by Kostrov [23], who proposed that the seismic strain rate is proportional to the sum of scalar seismic moments of all earthquakes in a given area. The seismic moment has been calculated from the body wave magnitude m_b. We use the Council of the National Seismic System (CNSS [24]) seismic catalogue, which has a good coverage of events with computed body wave magnitude for the period from 1963 to the present (Fig. 1). All the events of this catalogue that have saturated the body wave magnitude scale at 6.5 have been assigned recalculated m_b values compiled by Engdahl and Villaseñor [25]. In order to make the catalogue as complete as possible for large events, which release most of the seismic moment, we have included the five large events occurring in the area from 1900 to 1963 that are contained in the catalogue by Engdahl and Villaseñor [25]. When we calculate the seismic strain rate, we assume that each earthquake involves a strain rate effect that follows a Gaussian distribution. To avoid border effects, we have considered events occurring in an area 5° larger in each direction than that modelled.

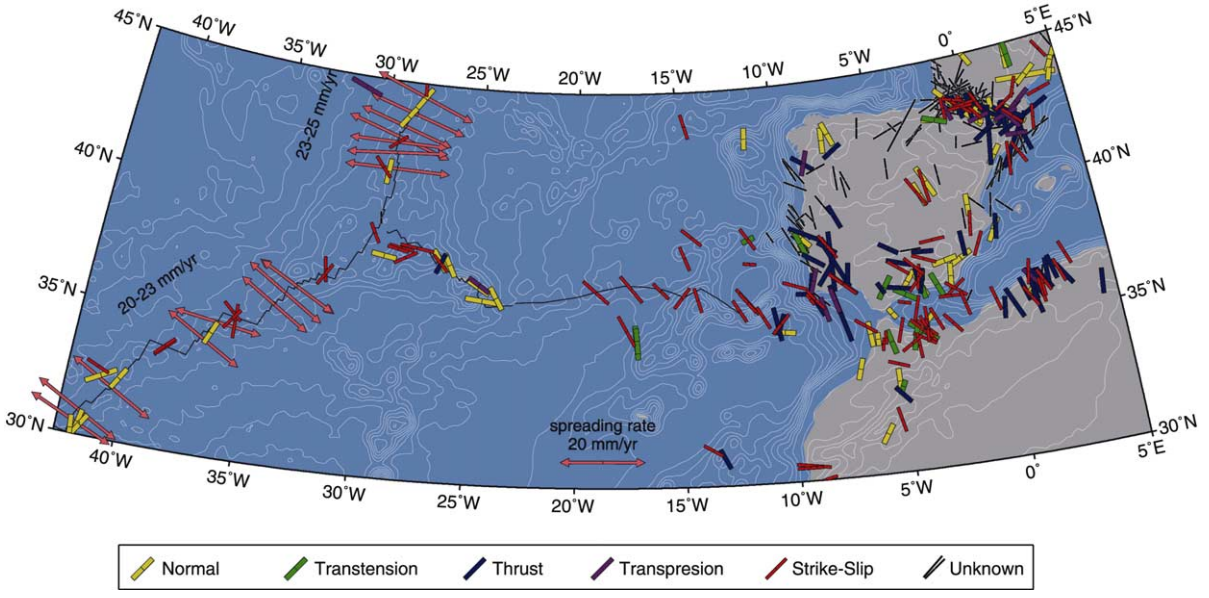

Fig. 3. Directions of the most compressive horizontal principal stress from the World Stress Map project (WSM2000[26]), Bezzeghoud and Buforn [8] and Borges et al. [27]. The colour of the symbol represents the tectonic regime and its length is proportional to the quality of data. Arrows represent Africa–North America and Eurasia–North America spreading rates obtained from the last 3 Ma and compiled by Argus et al. [21]. The isolines represent elevation every 500 m.

Some important limitations of the strain rate derived from earthquakes are that the seismicity measurements only cover a short period, and that it does not take into account ductile deformation. Therefore, we are not attempting to compare absolute values of model-predicted strain rate to seismic strain rate, but only their relative variations. We use the coefficient defined by Jiménez-Munt et al. [22] to test the correlation between the logarithms of the two smoothed strain rates.

Model-predicted principal stress orientations are compared to 364 data of the directions of maximum horizontal compression (Fig. 3). Most data (301 values) come from the most recent World Stress Map compilation (WSM2000 [26]). Sixty percent of these data are obtained from earthquake focal mechanisms; the rest use other types of stress indicators [26]. Additional data are taken from published studies and compilations of earthquake focal mechanisms with magnitude equal to or higher than 4 (e.g. [8,27]). All data include a quality coefficient describing the uncertainty associated with the stress orientation determination. We compute the mean misfit between the measured and the modelled azimuths of the most compressive horizontal principal stress, considering the deviation between the observed azimuth at a given site and the azimuths predicted at the closest nodes. The data have been weighted depending on the quality of the measurement. Taking into account the high scatter of stress azimuth data, that we are studying a large area with few measurements in some zones, and that they are often representative of local features not included in our models, the expected values of mean misfit are large, exceeding 30° [28].

Seafloor spreading rates compiled by Argus et al. [21] from magnetic anomalies (since 3 Ma) were also used to test model set 3_PLATES, in which we define fault elements along the Mid-Atlantic ridge. The scalar computed error corresponds to the RMS discrepancy from the 16 spreading rates available along the Mid-Atlantic ridge, from 30°N to 45°N. The modelled spreading rates are obtained from the difference of velocity imposed for the nodes along MAR belonging to North America and the velocity predicted for the nodes belonging to Eurasia and Africa plates (along MAR). Therefore, computed spreading rates depend not only on the western boundary condition, but also on the MAR friction coefficient.

Fig. 4 shows the results of scoring both model

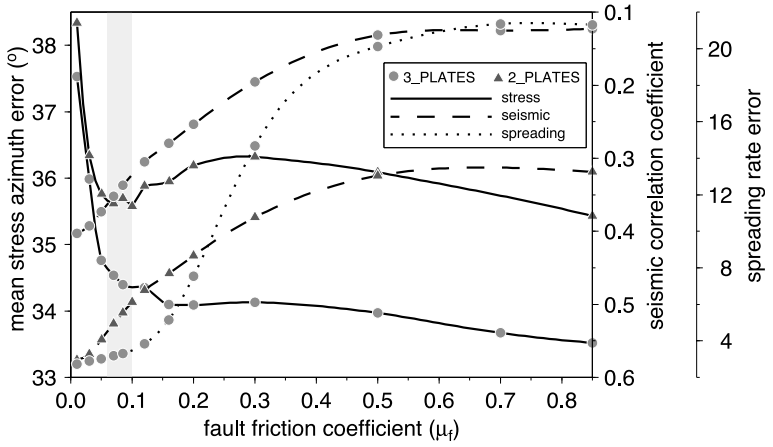

Fig. 4. Testable predictions as a function of the fault friction coefficient for the two models, 2_PLATES (triangles) and 3_PLATES (circles). Continuous lines represent the mean stress azimuth error, given by deviation of the maximum horizontal compression direction predicted by the model and the data. Broken lines represent the coefficient of strain rate correlation between the modelled and the seismic strain rates. Dotted lines the misfit between the Mid-Atlantic spreading rate data and the modelled values. Best models are those on the lower zone of the panel, with low mean stress azimuth and spreading rate error, but high correlation with the seismic strain rate. The grey strip indicates the range of optimum fault friction coefficients.

sets. Mean error in predicted stress azimuth varies from 33.5° to 38.3°, with lower values for model set 3_PLATES. The reason for this better fit is that the strong divergence caused by the boundary condition applied along the Mid-Atlantic ridge in 3_PLATES model (Fig. 2) forces the predicted most compressive horizontal principal stress directions to be nearly parallel to the ridge, in good agreement with stress data displayed in Fig. 3. On the other hand, a better correlation with the seismic strain rate is obtained with model set 2_PLATES. Actually, the high predicted strain rate along the ridge, which is a consequence of the high velocity applied there, is in contrast with the absence of large earthquakes occurring in the ridge area (where a large number of small earthquakes occur). This apparent mismatch can be understood by taking into account that, due to the high heat flow in this area, a significant part of the anelastic strain is expected to occur by ductile deformation, which is not included in computed seismic strain rates. Therefore, we give more weight to the scoring of stress directions and select 3_PLATES as our preferred model set.

Seafloor spreading rate error, computed only for model set 3_PLATES, reaches minimum values for very low fault friction coefficients and increases sharply for coefficients between 0.12 and 0.5. This error behaves similarly to the seismic correlation coefficient, in the sense of favouring models with very low fault friction. In contrast, misfit of stress azimuth data increases steeply for coefficients lower than 0.06. Considering the misfit to the three kinds of data, the best model is that with fault friction between 0.06 and 0.1. These friction coefficients are intermediate in value between the coefficient 0.03 for plate boundaries deduced from the global model of Bird [28] and the value 0.12 obtained by Jiménez-Munt et al. [9] for the transform plate boundary from eastern Azores to Gibraltar. These low fault friction coefficients are suspected to be related to anomalous pore pressure [14]. Figures in the following sections will show model predictions assuming a fault friction coefficient of 0.07, a value that represents the best model found in this study.

4.2. Surface velocity, fault slip rates and strain rate

Model-predicted surface velocities with respect to a fixed Eurasia plate are shown in Fig. 5. This figure provides a very clear image of the counterclockwise rotation of Africa and enables a simple explanation of the resulting tectonic regime all along the Africa–Eurasia plate boundary. In northern Algeria, convergence is almost completely absorbed in the area of the Tell Atlas front. Further to the west convergence is more distributed, between the Alboran ridge and the Rif and western Betics thrust front.

In the area of the Gulf of Cadiz and Gorringe Bank, deformation is also distributed and the Africa motion is partially transmitted to the southernmost Iberian Atlantic margin, resulting in velocity values of 1–2 mm yr^{-1}. Further to the west, the plate boundary absorbs almost entirely the relative plate motion, which is accommodated by right lateral motion along the strike-slip Gloria fault and by divergence with a component of right lateral motion along the Terceira ridge. A dense Global Positioning System (GPS) network recently established in the Azores Islands will soon be providing observations of the present-day pattern of deformation in this region that could be compared to model predictions [29]. The outwards velocity applied to the external nodes of fault elements along the Mid-Atlantic ridge does not affect noticeably the interior of the plates and it is therefore expected to cause strong divergence concentrated along the ridge.

Fig. 5 also shows the geodetic data set corresponding to seven sites located in the Iberian Peninsula. The horizontal velocities for these sites are derived by the Matera Geodesy Center of the Italian Space Agency (ASI-CGS) from independent space geodetic solutions using GPS, Satellite Laser Ranging (SLR) and Very Long Baseline Interferometry (VLBI) data [30,31]. The independent geodetic solutions have been obtained by analysing almost all the data available in the central Mediterranean. Each solution has been unconstrained and combined with the others, with no need to introduce any reference system to constrain the final solution. Geodetic data shown in

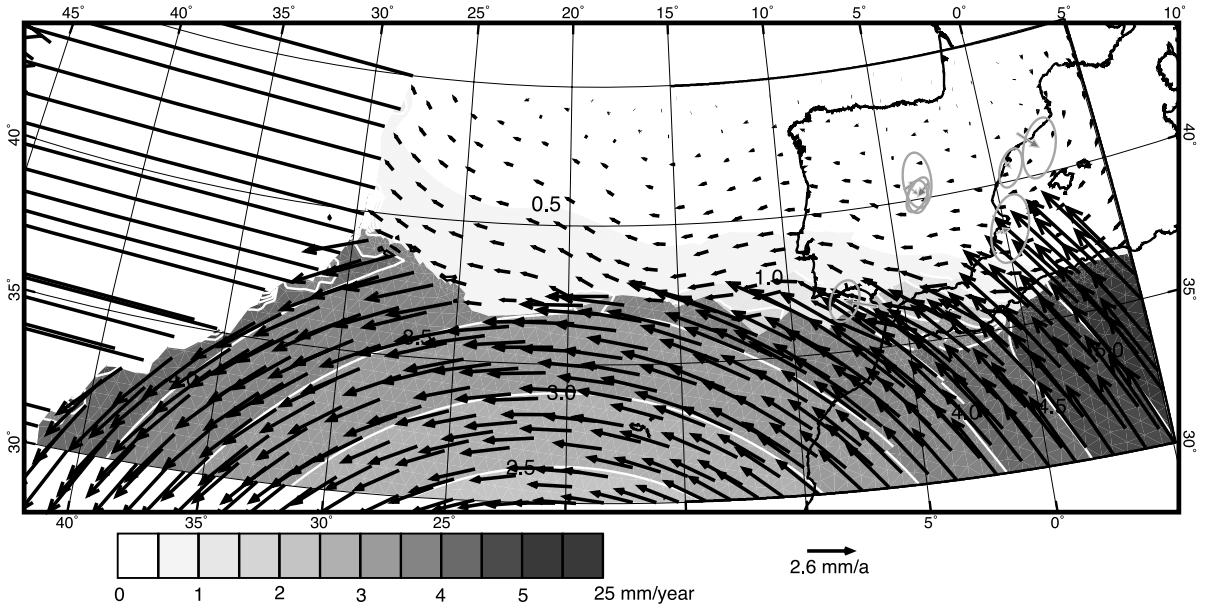

Fig. 5. Horizontal velocity field from the 3_PLATES model set with a fault friction coefficient of 0.07. Isolines every 0.5 mm yr^{-1}. The geodetic solutions (grey arrows) with their uncertainties obtained for seven sites located in the Iberian Peninsula are also shown [30,31].

Fig. 5 indicate residual velocities with respect to central Europe, where the Euler pole of the rotation vector has been estimated using a subset of 22 stable Eurasian sites. The large error ellipses in the Iberian Peninsula indicate that geodetic data are still sparse and highly variable in this zone. Two general features of data are correctly reproduced by model predictions: the low velocities in the central and eastern Iberian Peninsula, and the higher velocity of 2–3 mm yr^{-1} in WNW direction obtained in southern Iberia. However, keeping in mind the large uncertainties associated with geodetic data and the model limitations, we do not intend at this stage to fit these data, but to show the capability of this kind of modelling to generate a number of predictions that are testable by future data acquisition.

In order to evaluate possible ridge push effects we performed a test in which no boundary condition representing plate motion was applied, so that we can consider only motion caused by forces due to lateral variations of potential energy. We deduce that these variations cause negligible eastward horizontal velocities, lower than 0.005 mm yr^{-1}. Furthermore, the integrated pressure exerted by the Iberian Peninsula and northern Africa on the surrounding margins causes velocities comparable to or even higher than those related to the ridge stress anomaly.

Fig. 6 shows model-predicted long-term average fault slip rates. Including such a wide zone of the Africa–Eurasia plate boundary permits us to reproduce the progressive change of tectonic regime from thrusting in the Tell Atlas, through transpression in the Gorringe–Gulf of Cadiz–Alboran region, pure right lateral motion of the strike-slip Gloria Fault, and transtension in the Terceira ridge [4–6,32]. Shortening rates of 3–5 mm yr^{-1} (obtained by multiplying slip rates of low angle faults by cos 25°) have been obtained along the Tell Atlas front. These values of slip rates must be considered an upper bound since we have probably exaggerated the continuity of the modelled Tell Atlas front. Actually, NE–SW striking thrust faults in this region often show a right lateral en echelon pattern, suggesting that they are likely connected at depth by E–W strike-slip faults [33]. However, for simplicity,

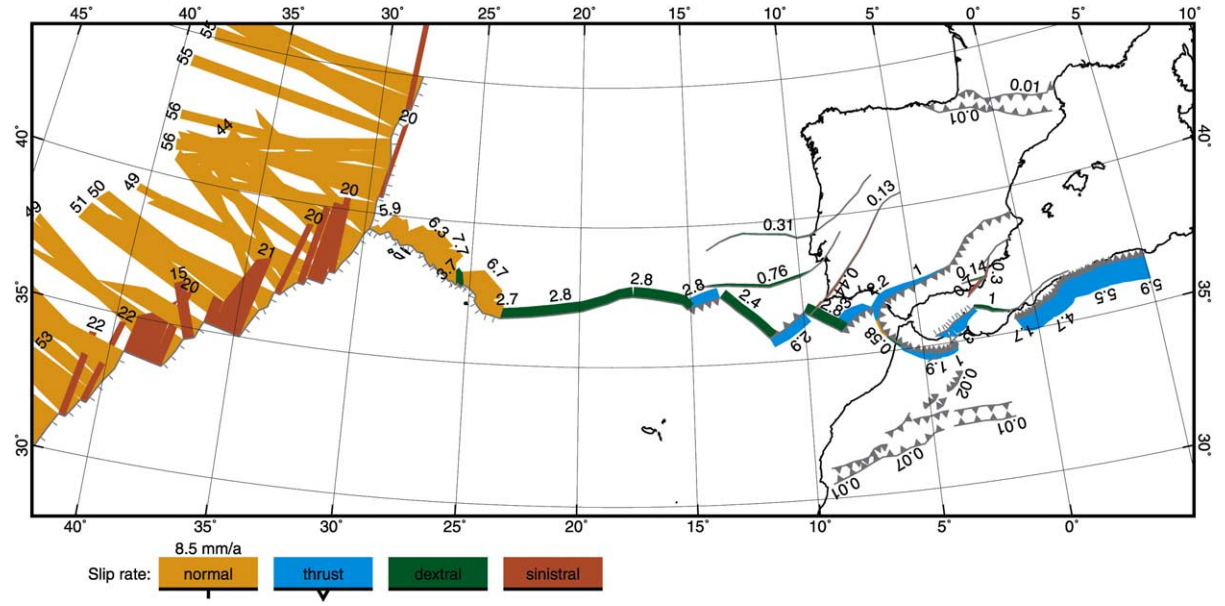

Fig. 6. Fault slip rates and tectonic regime from the 3_PLATES model set with a fault friction coefficient of 0.07.

we have introduced a long, continuous, low-angle fault without short vertical fault segments. Nonetheless, the predicted shortening rates fall between the 5 mm yr^{-1} proposed by Dewey [34] for the last 9 Ma, and 2.3 mm yr^{-1} deduced by Meghraoui et al. [33] for Quaternary compressional structures.

Further to the west, predicted fault slip is quite homogeneously distributed along the Alboran Sea faults and the modelled Betic–Rif thrust front, except on the eastern Betic front, which the model shows to be inactive. The general trend of predicted fault slip directions in the continental domain (between 0° and 13°W) is consistent with geological indications. Vertical NE–SW trending faults are predicted to have sinistral motion (e.g. the Alhama–Palomares–Carboneras fault system), while E–W to NW–SE striking faults are predicted to have dextral motion (e.g. the Yussuf fault and the vertical fault zones connecting the Guadalquivir Bank, Gorringe Bank and northern Madeira Tore Rise).

Maximum predicted fault shortening rates of about 1.3 mm yr^{-1} in the Rif are consistent with the rates of 1–2.3 mm yr^{-1} estimated in the area by Meghraoui et al. [33]. These relatively high fault slip rates seem to be inconsistent with the lack of thrust earthquakes in the Rif area. However, we cannot reject model results since the time span of calculated focal mechanisms may be shorter than the recurrence period of moderate size thrust events. In fact, historical data together with field work and air photo interpretation led Piccardi et al. [35] to propose activation of E–W oriented thrusts (just south of the main frontal thrust of the Rif) as the most probable cause of the 1755 Meknes earthquake (Morocco).

In the oceanic domain (west of the Madeira Tore Rise) we obtain uniform slip rates of 2.6–2.8 mm yr^{-1} along the vertical strike-slip Gloria fault. High angle faults along the Terceira ridge are predicted to slip in a normal sense with a component of right lateral motion. Our results are therefore in agreement with a number of seismotectonic studies (e.g. [4,5]) that infer a change from right lateral motion in the Gloria fault to transtension in the Terceira ridge. Maximum predicted extensional rates (computed as the product of slip rate and cos 65°) in the Terceira ridge are 3.1 mm yr^{-1}. The predicted values are somewhat lower than the relative plate velocities of 4 ± 1 mm

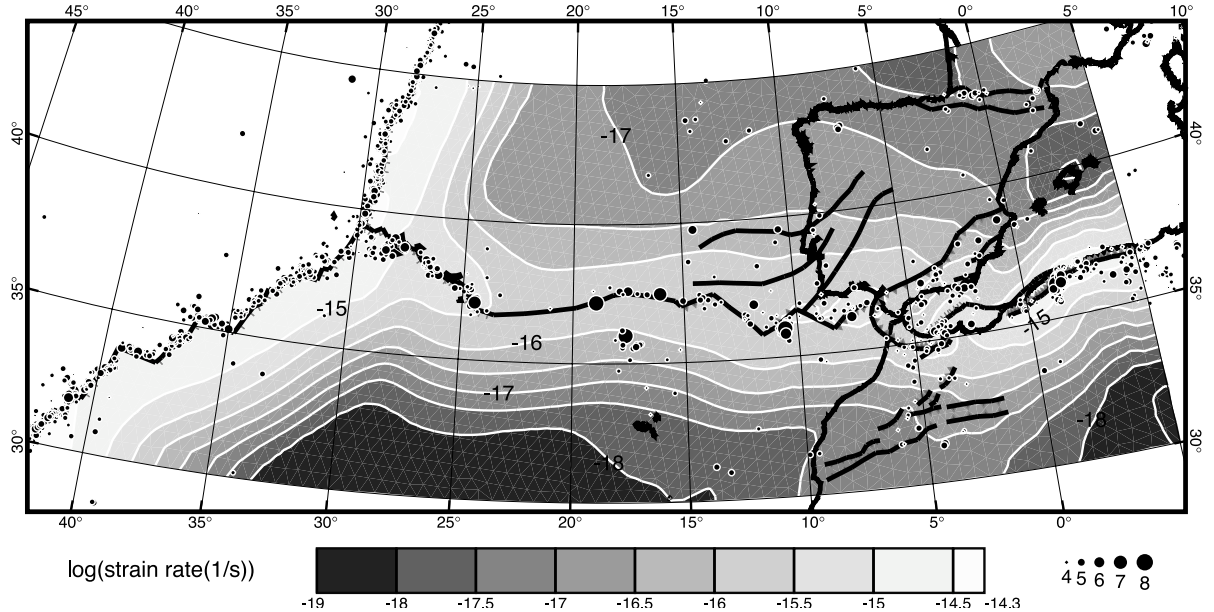

Fig. 7. Common logarithm of the smoothed strain rate from the 3_PLATES model set with a fault friction coefficient of 0.07. For comparison with seismic strain rate we also display earthquakes of magnitude m_b equal to or larger than 4 (circles), from the CNSS [24] seismic catalogue.

yr^{-1} for the Gloria fault and 4.9 mm yr^{-1} for the Azores obtained by DeMets et al. [36] using seafloor spreading, transform azimuths and earthquake slip vectors. Model predicted fault slip rates along the Mid-Atlantic ridge vary between 55–56 mm yr^{-1} to the north of the Azores Islands and 46–53 mm yr^{-1} to the south, which correspond to spreading rates of about 24 mm yr^{-1} and 19.5–22 mm yr^{-1}, respectively. This result is consistent with the observed slightly lower spreading rates south of the Azores [21] (Fig. 3).

The different deformational styles seem to be related to the different types of lithospheres in contact at the plate boundary. Deformation tends to concentrate and to define a narrow plate boundary at the contact between continental lithosphere and a young oceanic basin (at the Tell Atlas front), and at the contact between two oceanic lithospheres (west of the Madeira Tore Rise). In contrast, we obtain widespread deformation in the area of continent–continent convergence. Model results are therefore consistent with the general concept that oceanic lithosphere is more stable and tectonic activity is largely restricted to a well-defined plate boundary.

Fig. 7 shows the common logarithm of the smoothed strain rate obtained with our best model. For qualitative comparison with the seismic strain rate, we also display earthquakes with magnitude 4 or greater. The smoothed strain rate includes both the contributions from fault slip and anelastic deformation within the continuum blocks. The areas of maximum model-predicted strain rate are northern Algeria and the Mid-Atlantic ridge. The former prediction is in good agreement with the intense seismic activity of the area. However, the high fault slip rate along the Mid-Atlantic and Terceira ridges (Fig. 6) results in an elevated strain rate there, which is in contrast to the moderate magnitude of earthquakes in these areas. As previously mentioned, due to the high heat flow of these areas (Fig. 2) an important part of the anelastic strain may not be expressed as earthquakes, but likely occurs by ductile deformation.

The relatively high strain rate in the southern

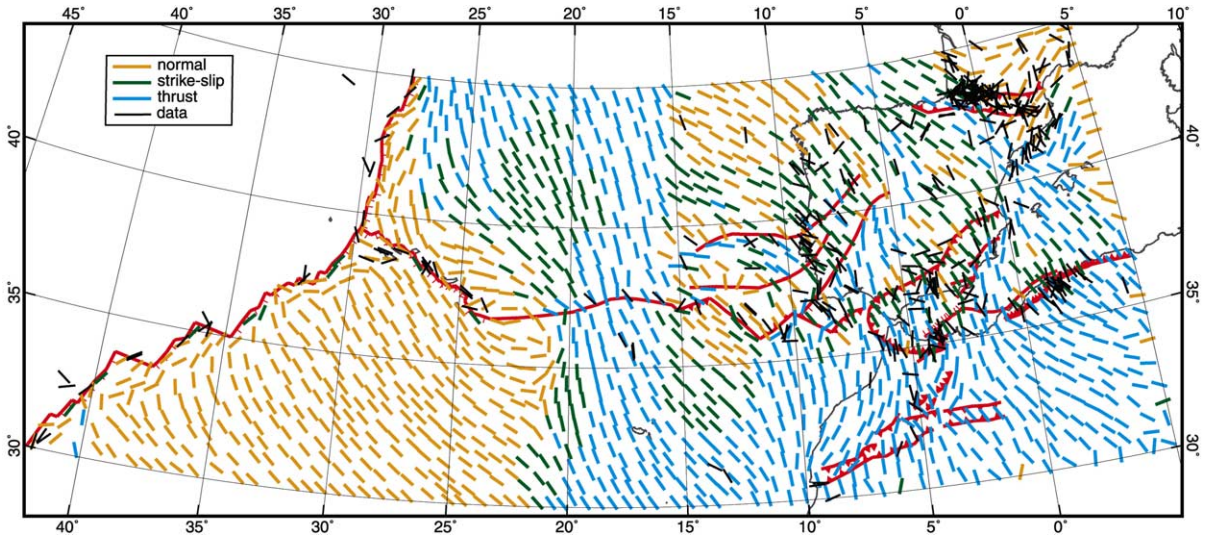

Fig. 8. Most compressive horizontal principal stress direction from the 3_PLATES model set with a fault friction coefficient of 0.07. Colour indicates tectonic regime. Black symbols indicate data of directions of the most compressive horizontal principal stress.

Alboran Sea, northeastern Morocco and Gulf of Cadiz is consistent with the significant seismicity in these areas. Our best model predicts a uniform strain rate distribution along the transform segment of the plate boundary (from 15°W to 24°W), which is in disagreement with the absence of seismicity in the Gloria fault and with the accumulation of large magnitude earthquakes in the eastern part of this segment (from 15°W to 19°W). Taking into account that warmer areas such as the Mid-Atlantic ridge do have significant seismicity, it seems unrealistic that strain is completely accommodated in the area by ductile flow. In our opinion, the lack of seismicity of the Gloria fault could be a transient effect of elastic strain accumulation and therefore cannot be properly reproduced by our model of steady velocity averaged over several seismic cycles. Studies of historical seismicity would be very useful in providing a complete image of the seismic behaviour of the Gloria fault. We can infer from our modelling that the long-term seismic hazard of the Gloria fault is similar to that of the adjacent transform segment of the plate boundary. This can have important consequences in the hazard assessment of the area, given the proximity of the Azores Islands.

4.3. Stress directions

Fig. 8 shows the model-predicted directions of maximum horizontal compression and tectonic regime. This model properly reproduces the regional trend of stress orientation data and tectonic regime (Fig. 3). The stress regime changes in the Ibero–Maghrebian region, from thrusting and strike-slip in the Tell Atlas to predominant strike-slip in the Betics, central Alboran Sea and eastern Rif, in agreement with focal mechanisms of earthquakes studies (e.g. [7,8]). Reilly et al. [37] deduce, on the basis of geodetic measurements in the Strait of Gibraltar, maximum shortening in E–W direction and dilatation in N–S direction. This result is in contrast with maximum NNW–SSE horizontal compression predicted for this area. Keeping in mind that the predicted direction of compression in this area is consistent with regional direction of convergence between Africa and Eurasia, the discrepancy between the results by Reilly et al. [37] and the present study could be attributed to local effects.

The predicted compressive axes in the Iberian Peninsula are oriented in the NNW–SSE to NW–SE direction, as deduced from geologic and seismotectonic studies (e.g. [11,27,38]), except for the

eastern Pyrenees, where compression changes to NE–SW direction, in good agreement with stress data (Fig. 3). Model predictions for the area of Galicia (northwestern Spain) are consistent with the focal mechanism solutions of the seismic activity that occurred in the area between November 1996 and May 1997, with more than 250 events with magnitudes m_b ranging form 3.0 to 5.1. These mechanisms indicate normal faulting and compressive axes oriented in NNW–SSE direction (Fig. 3), in agreement with model predictions. Modelled faults in the western Iberian Peninsula cause a rotation to the west of the compressive stress directions, the western component increasing towards the Iberian Atlantic margin. Another feature of stress data that is successfully reproduced by our model is the change from NNE–SSW orientation of the compressive axes in the Atlas to NNW–SSE compression in the Mediterranean coast of Morocco.

In the area between the Madeira Tore Rise and the Gulf of Cadiz, predicted compressive axes are oriented parallel to vertical faults and perpendicular to low-angle faults, thus resulting in transpression of this area. Further to the west we obtain a progressive counterclockwise rotation of the compressive axes from east to west until they become roughly parallel to the Terceira ridge. The tectonic regime predicted for this area is consistent with seismotectonic studies that indicate predominant normal faulting with horizontal tensions on average in a N25°E direction [5]. Predicted directions of maximum horizontal compression in the Mid-Atlantic ridge are roughly parallel to the ridge with a regime of normal faulting, in agreement with stress data. This feature is not satisfactorily reproduced by model set 2_PLATES, where predicted compressive axes are perpendicular to the ridge, giving a higher misfit between the measured and the modelled directions of the most compressive horizontal principal stress (Fig. 4).

5. Conclusions

Using the thin-shell approach, we have successfully reproduced the main characteristics of the present-day tectonic regime and strain field in the part of the Africa–Eurasia plate boundary running between the Mid-Atlantic ridge and Tell Atlas. We have been able to represent the relative motion between North America, Africa and Eurasia by defining fault elements along the modelled Mid-Atlantic ridge (model set 3_PLATES) and applying relative plate velocity boundary conditions. Including the Mid-Atlantic ridge has also permitted us to deduce that the effect of the ridge push on the continental lithosphere is negligible. We deduce that lateral density variations on the ridge cause negligible eastward horizontal velocities, which are counteracted by westward-directed velocities caused by the integrated pressure exerted by the Iberian Peninsula and northern Africa on their Atlantic margins.

The velocity boundary condition representing spreading on the Mid-Atlantic ridge is shown to have negligible influence in the interior of the plates and to produce strong divergence concentrated along the ridge. However, this condition is necessary to properly reproduce the observed directions of maximum horizontal compression on the Mid-Atlantic ridge.

The best model scores have been obtained with fault friction coefficients as low as 0.06–0.1, a value lower than the coefficient 0.12 obtained for the transform segment of the plate boundary from the eastern Azores to Gibraltar [9].

In spite of the complex tectonic regime of the study area, we have properly reproduced the progressive change from thrusting in the Tell Atlas, through combined thrusting in the Betic–Rif thrust front and transpression in the Gorringe–Gulf of Cadiz–Alboran region, pure right lateral motion of the strike-slip Gloria Fault, and transtension in the Terceira ridge. The predicted compressive axes in the Iberian Peninsula are oriented in the NNW–SSE to NW–SE direction, except for the eastern Pyrenees, where compression changes to NE–SW direction, in good agreement with stress data.

Model-predicted strain rates and fault slip rates along the Gloria fault are similar to those of the adjacent transform segment of the plate boundary, which is marked by an alignment of large earthquakes. We therefore infer a significant

long-term seismic hazard for the Gloria fault, and interpret the absence of seismicity on this fault as possibly due to transient elastic strain accumulation.

The different deformational styles seem to be related to the different types of lithosphere in contact at the plate boundary. Deformation tends to concentrate so as to define a narrow plate boundary in the contact between continental lithosphere and a young oceanic basin (at the Tell Atlas front), and in the contact between two oceanic lithospheres (west of the Madeira Tore Rise). In contrast, our best model predicts widespread deformation in the area of continent–continent convergence.

This modelling is useful to provide a number of testable predictions that could be compared to future data acquired in ongoing research projects. In particular, high-accuracy geodetic measurements in the Azores Islands and Iberian Peninsula will be extremely useful to constrain the present-day pattern of deformation of these areas.

Acknowledgements

We acknowledge the editor S. King and the reviewers P. Lundgren, R. Russo and R. Govers for their efforts in improving the manuscript. The authors acknowledge Peter Bird (University of California Los Angeles, UCLA) for making available thin-shell and graphic programs, and for providing extensive documentation and assistance. We are grateful to the Council of the National Seismic System (CNSS) for making available the seismic catalogue. The authors thank A. Udías, E. Buforn (University Complutense of Madrid), Antonio Villaseñor (University of Utrecht) and Roberto Sabadini (University of Milan) for constructive comments. We thank Roberto Devoti and the ASI-CGS group for their geodetic solution and support. The Italian Ministry of University and Scientific Research (COFIN2000 and ASI-1998-2000-Working group) and the Spanish Ministry of Science and Technology (Ramon y Cajal program and project BTE2002-02462) partially supported this work.*[SK]*

References

[1] K.D. Klitgord, H. Schouten, Plate kinematics of the central Atlantic. In: P.R. Vogt, B.E. Tucholke (Eds.), The Geology of North America, Vol. M, The Western North Atlantic Region, Geol. Soc. Am., Boulder, CO, 1986, pp. 351–378.

[2] S.P. Srivastava, W.R. Roest, L.C. Kovacs, G. Oakey, S. Lévesque, J. Verhoef, R. Macnab, Motion of the Iberia since the Late Jurassic: results from detailed aeromagnetic measurements in the Newfoundland Basin, Tectonophysics 184 (1990) 229–260.

[3] R. Searle, Tectonic pattern of the Azores spreading centre and triple junction, Earth. Planet. Sci. Lett. 51 (1980) 415–434.

[4] N. Grimison, W. Chen, The Azores-Gibraltar plate boundary: focal mechanisms, depths of earthquakes, and their tectonic implications, J. Geophys. Res. 91 (1986) 2029–2047.

[5] E. Buforn, A. Udías, M.A. Colombás, Seismicity, source mechanisms and tectonics of the Azores-Gibraltar plate boundary, Tectonophysics 152 (1988) 89–118.

[6] J.L. Morel, M. Meghraoui, Gorringe-Alboran-Tell tectonic zone: a transpression system along the Africa-Eurasia plate boundary, Geology 24 (1996) 755–758.

[7] A. Calvert, F. Gómez, D. Seber, N.J. Barazangi, A. Ibenbrahim, A. Demnati, An integrated geophysical investigation of recent seismicity in the Al-Hoceima Region of North Morocco, Bull. Seismol. Soc. Am. 87 (1997) 637–651.

[8] M. Bezzeghoud, E. Buforn, Source parameters of the 1992 Melilla (Spain, $M_w = 4.8$), 1994 Alhoceima (Morocco, $M_w = 5.8$), and Mascara (Algeria, $M_w = 5.7$) earthquakes and seismotectonic implications, Bull. Seismol. Soc. Am. 89 (1999) 359–372.

[9] I. Jiménez-Munt, P. Bird, M. Fernàndez, Thin-shell modeling of neotectonics in the Azores-Gibraltar region, Geophys. Res. Lett. 28 (2001) 1083–1086.

[10] A.M. Negredo, P. Bird, C. Sanz de Galdeano, E. Buforn, Neotectonic modeling of the Ibero-Maghrebian region, J. Geophys. Res. (2002) in press.

[11] M. Herraiz, G. deVicente, R. Lindo-Ñaupari, J. Giner, J.L. Simón, J.M. González-Casado, O. Vadillo, M.A. Rodríguez-Pascua, J.I. Cicuéndez, A. Casas, L. Cabañas, P. Rincón, A.L. Cortés, M. Ramírez, M. Lucini, The recent (upper Miocene to Quaternary) and present tectonic stress distributions in the Iberian Peninsula, Tectonics 19 (2000) 762–786.

[12] X. Kong, P. Bird, SHELLS: a thin-plate program for modeling neotectonics of regional or global lithosphere with faults, J. Geophys. Res. 100 (1995) 22129–22131.

[13] P. Bird, Thin-plate and thin-shell finite element programs for forward dynamic modeling of plate deformation and faulting, Comput. Geosci. 25 (1999) 383–394.

[14] P. Bird, X. Kong, Computer simulations of California tectonics confirm very low strength of major faults, Geol. Soc. Am. Bull. 106 (1994) 159–174.

[15] S.H. Kirby, Rheology of the lithosphere, Rev. Geophys. 21 (1983) 1458–1487.
[16] E. Gràcia, J.J. Dañobeitia, J. Vergés, R. Bartolomé, D. Córdoba, The structure of the Gulf of Cadiz (SW Iberia) imaged by new multi-channel seismic reflection data, Geophys. Res. Abstr. 2 (2000) 61.
[17] H.N. Pollack, S.J. Hurter, J.R. Johnson, Heat loss from the Earth's interior: analysis of the global data set, Rev. Geophys. 31 (1993) 267–280.
[18] M. Fernàndez, I. Marzán, A. Correia, E. Ramalho, Heat flow, heat production, and lithospheric thermal regime in the Iberian Peninsula, Tectonophysics 291 (1998) 29–53.
[19] B. Parsons, J.G. Sclater, An analysis of the variation of ocean floor bathymetry and heat flow with age, J. Geophys. Res. 82 (1977) 803–827.
[20] M. Torne, M. Fernàndez, M.C. Comas, J.I. Soto, Lithospheric structure beneath the Alboran basin: results from 3D gravity modeling and tectonic relevance, J. Geophys. Res. 105 (2000) 3209–3228.
[21] D.F. Argus, R.G. Gordon, C. DeMets, S. Stein, Closure of the Africa-Eurasia-North America plate motion circuit and tectonics of the Gloria fault, J. Geophys. Res. 94 (1989) 5585–5602.
[22] I. Jiménez-Munt, M. Fernàndez, M. Torne, P. Bird, The transition from linear to diffuse plate boundary in the Azores-Gibraltar region: results from a thin-sheet model, Earth. Planet. Sci. Lett. 192 (2001) 175–189.
[23] V. Kostrov, Seismic moment and energy of earthquakes, and seismic flow of rock, Izv. Acad. Sci. USSR Phys. Solid Earth 1 (1974) 23–44.
[24] CNSS, Council of National Seismic System (1898–present), http://quake.geo.berkeley.edu/cnss/catalog-search.html.
[25] E.R. Engdahl, A. Villaseñor, Global Seismicity: 1900–1999, in: W.H.K. Lee, H. Kanamori, P.C. Jennings, C. Kisslinger (Eds.), International Handbook of Earthquake and Engineering Seismology, Part A, Ch. 41 Academic Press, San Diego (2002) pp. 665–690.
[26] B. Mueller, J. Reinecker, O. Heidbach, K. Fuchs, The 2000 release of the World Stress Map (available online at www.world-stress-map.org), 2000.
[27] J.F. Borges, A.J.S. Fitas, M. Bezzeghoud, P. Teves-Costa, Seismotectonics of Portugal and its adjacent Atlantic area, Tectonophysics 337 (2001) 373–387.
[28] P. Bird, Testing hypotheses on plate-driving mechanisms with global lithosphere models including topography, thermal structure, and faults, J. Geophys. Res. 103 (1998) 10115–10129.
[29] R. Fernandes, B. Ambrosius, R. Noomen, L. Bastos, J. Osorio, P. Baptista, Behavior of the Eurasian, North American and African plates in the Azores region, 10th General Assembly of the WEGENER Project, San Fernando, Spain, 18–22 September 2000.
[30] R. Devoti, L. Ferraro, R. Lanotte, C. Luceri, V. Sciarretta, G. Bianco, Combined velocity solution in the Central Mediterranean area obtained from space geodetic networks, 11th General Assembly of the WEGENER Project, Athens, Greece, 12–14 June 2002.
[31] ASI-CGS group, Geodaf The Mediterranean solution (ASImed). Current version: ASImed_VSG2002v01, http://geodaf.mt.asi.it/html/ASImed/ASImed.html (2002).
[32] A. Kiratzi, C.B. Papazachos, Active crustal deformation from the Azores triple junction to the Middle East, Tectonophysics 243 (1995) 1–24.
[33] M. Meghraoui, J.L. Morel, J. Andrieux, M. Dahmani, Tectonique plio-quaternaire de la chaîne tello-rifaine et de la mer d'Alboran: une zone complexe de convergence continent-continent, Bull. Soc. Géol. Fr. 167 (1996) 141–157.
[34] J.F. Dewey, M.L. Helman, E. Turco, D.H.W. Hutton, S.D. Knott, Kinematics of the Western Mediterranean, In: M.P. Coward, D. Dietrich, R.G. Park (Eds.), Alpine Tectonics, Spec. Publ. Geol. Soc. London 45 (1989) 265–283.
[35] L. Piccardi, G. Moratti, G. Vannucci, M. Dahmani, A. Bendkik, M. Chenakeb, The 1755 'Meknes' earthquake (Morocco), in: Workshop on the Geodynamics of the Western Part of Eurasia-Africa Plate Boundary (Azores-Tunisia), Extended Abstr. Book, San Fernando, Spain, 2001.
[36] C. DeMets, R.G. Gordon, D.F. Argus, S. Stein, Current plate motions, Geophys. J. Int. 101 (1990) 425–478.
[37] W.I. Reilly, G. Fredrich, G.W. Hein, H. Landau, J.L. Almazan, J.L. Caturla, Geodetic determination of crustal deformation across the Strait of Gibraltar, Geophys. J. Int. 111 (1992) 391–398.
[38] A. Ribeiro, J. Cabral, R. Baptista, L. Matias, Stress pattern in Portugal mainland and the adjacent Atlantic region, West Iberia, Tectonics 15 (1996) 641–659.